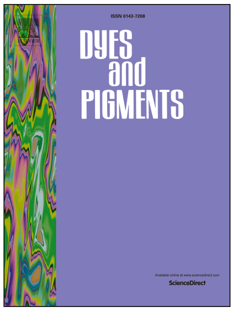

Alkyl chain-dependent cyano-stilbene derivative's molecular stacking, emission enhancement and fluorescent response to the mechanical force and thermal stimulus

Pengchong Xue, Chunyu Zhang, Kunpeng Wang, Meng Liang, Tong Zhang

PII: S0143-7208(18)32533-6

DOI: https://doi.org/10.1016/j.dyepig.2018.12.036

Reference: DYPI 7241

To appear in: *Dyes and Pigments*

Received Date: 19 November 2018

Revised Date: 17 December 2018

Accepted Date: 17 December 2018

Please cite this article as: Xue P, Zhang C, Wang K, Liang M, Zhang T, Alkyl chain-dependent cyano-stilbene derivative's molecular stacking, emission enhancement and fluorescent response to the mechanical force and thermal stimulus, *Dyes and Pigments* (2019), doi: https://doi.org/10.1016/j.dyepig.2018.12.036.

Graphic abstract

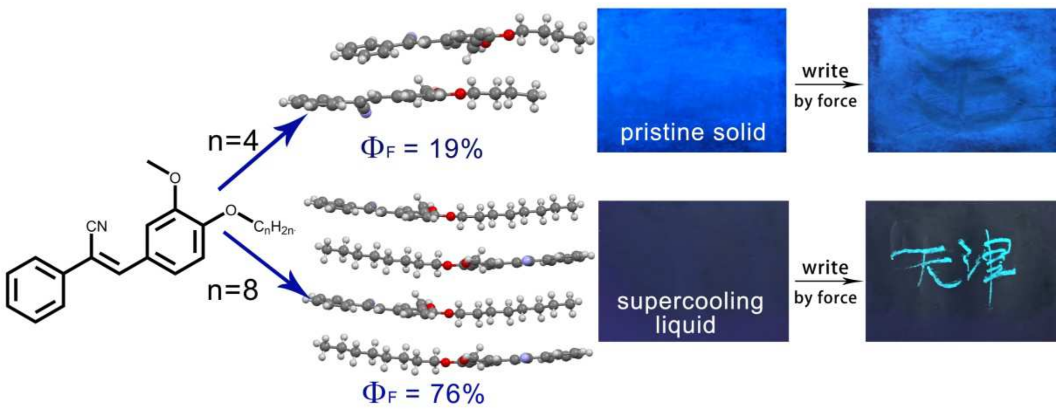

Both cyano-stilbene derivatives exhibited crystallization-induced emission enhancement and the length alkyl chains determined in luminescent efficiency and mechanochromism.

Alkyl chain-dependent cyano-stilbene derivative's molecular stacking, emission enhancement and fluorescent response to the mechanical force and thermal stimulus

Pengchong Xue,* Chunyu Zhang, Kunpeng Wang, Meng Liang, Tong Zhang

Tianjin Key Laboratory of Structure and Performance for Functional Molecules, Key Laboratory of Inorganic-Organic Hybrid Functional Material Chemistry, Ministry of Education, College of Chemistry, Tianjin Normal University
No. 393 Bin Shui West Road, Tianjin, 300387, P. R. China.
E-mail: xuepengchong@126.com.

Abstract: Two cyano-stilbene derivatives with butyl (C4MPA) and octyl groups (C8MPA) were synthesized to investigate the effects of alkyl chains on molecular stacking, emission enhancement, and mechanofluorochromism. The two compounds displayed weak emissions in monomolecular state and emitted an enhanced fluorescence in crystal state. However, the fluorescence quantum yield of C4MPA (19%) was lower than that of C8MPA (76%). Face-to-face dimer stacking was found only in the C4MPA crystal, in which molecules adopted a nonplanar configuration. The C8MPA crystal presented two kinds of antiparallel 1D arrangement. One involved the antiparallel stacking of nonplanar aromatic moieties. The other consisted of coplanar molecules without π-π stacking, which were responsible for the higher luminescence yield. Moreover, the emission of the C4MPA solid was quenched under mechanical force, whereas the C8MPA solid still emitted a strong fluorescence after grinding. C8MPA lost fluorescence when heated at above 60 °C because of its low melting point, and the supercooling viscous liquid without fluorescence was observed even the sample was cooled to room temperature for 10 h, meaning a very slowly crystallization process. Such non-emissive supercooling viscous liquid might rapidly transform into strongly emissive solid under the mechanical force shearing stimulus. Thus, C8MPA films could be used as sensors for mechanical force and thermal stimuli.

Introduction

Stimuli-responsive organic materials have attracted considerable interest and have been extensively utilized in advanced applications in various sensors,[1] electronic skin,[2] drug delivery,[3] self-healing materials,[4][5] molecular motor,[6] and so on. In particular, organic luminescence materials that respond to mechanical force have been rapidly developed because of their wide applications in sensors, memory chips, and security inks.[7][8][9][10][11][12][13] These smart materials exhibit mechanochromism (MC), which refers to their ability to change their emission color and intensity after an appropriate external stress was applied.[14][15][16] The molecular structures of these smart materials consist of pure organic molecules and metal complexes. Almost pure MC organic molecules emit fluorescence and exhibit mechanofluorochromic (MFC) behavior.[17][18] By contrast, metal complexes with Pt(II), Au(I), Cu(I), and Ir(III) generally exist in an excited triplet state and possess large shifts of emission wavelength because of the alteration of the metal–metal interaction triggered by the mechanical force stimuli.[19][20][21] To date, many kinds of pure organic MC molecules, including tertraphenylethene, [22][23] 9,10-divinylanthracene, [24][25] triphenylamine,[26][27] phenothiazine,[28][29][30] β-diketone boron complexes,[31][32] diiodo boron diiminates,[33] and cyano-ethylene,[33][34] have been found to exhibit obvious MFC behavior. The results suggested that non-planar geometry and electron pull–push structure can typically change the luminescence color under a mechanical force.

MFC materials with an aggregation-induced emission (AIE) were rapidly developed because they emitted an enhanced fluorescence in solid state and were non-emissive in solution or melted state.[35][36][37] If an AIE molecule possesses a low melting point it is possible for molecule to have a slow crystallization rate and then would like to exhibit mechanical force-induced luminescence enhancement (MILE) properties.[38][39][40][41] In other words, a non-emissive supercooling solid or liquid will transform into a strongly emissive solid under a mechanical force stimulus due to mechanical force-induced crystallization. However, such functional organic molecules still are rare. In this case, two cyano-stilbene derivatives with butyl (C4MPA) and octyl groups (C8MPA) were synthesized in the prospect of obtaining MILE molecules. Their photophysical, MFC, and MILE properties have been investigated. It was found that both two compounds were AIE molecule. C4MPA exhibited emission quenching after grinding, whereas C8MPA did not change its fluorescence intensity and color. More interestingly, C8MPA displayed a low melting point and a slow crystallization rate, both of which promoted the MILE behavior of C8MPA. The supercooling C8MPA viscous liquid was non-emissive, and strongly fluorescent crystals formed under the mechanical force stimulus. Thus, the luminescence pattern on a supercooling film could be drawn by a round pen. Moreover, non-emissive patterns were also written by a hot pen. These patterns would automatically disappear or self-erase and could be written repeatedly.

Results and discussion

Photophysical properties in solutions

First, their photophysical properties in solution were investigated. The two compounds were colorless and easily dissolved in common solvents, such as hexane, CH_2Cl_2, THF, acetone, DMF, and DMSO, to form colorless solutions. They have similar absorption and emission spectra in different solvents. Fig. 1 shows the absorption and fluorescence spectra of C4MPA. The maximal absorption peak was located at 348 nm in cyclohexane, which shifted to 351 nm in CH_2Cl_2, and 355 nm in polar DMF. Moreover, the emission band possessed red shifts in polar solvents. For instance, C4MPA had an emission peak at 400 nm in cyclohexane and 408 nm in CH_2Cl_2, which slightly red-shifted to 414 nm. Such small shifts of the emission spectra in polar solvents suggest that the polarities of C4MPA in excited and ground state have small difference.[42][43] Moreover, it was found that two compounds emitted very weak fluorescence in different solvents. For example, the fluorescence quantum yields of C4MPA and C8MPA in cyclohexane are 0.1% and 0.09%, respectively.

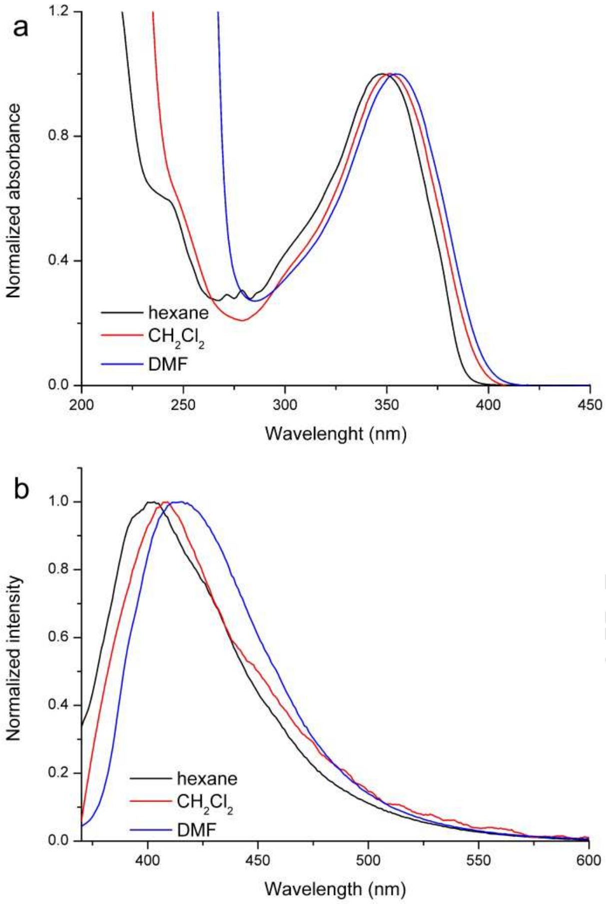

Fig. 1 (a) Absorption (b) emission spectra of C4MPA in different solvents.

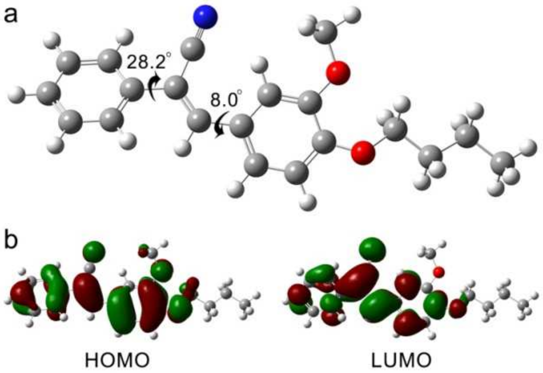

Fig. 2 (a) Optimal geometry of **C4MP**A with twisted angles and (b) corresponding frontier orbital (HOMO and LUMO) distributions.

To elucidate the emission spectra in different solvents, quantum chemical calculation was performed by density functional theory calculations at the B3LYP/6-31G(d) level. As shown in Fig. 2b, the HOMO state density was uniformly distributed at the whole aromatic unit, and the LUMO state density at two oxygen atoms was reduced. Moreover, time-dependent DFT calculation derived an electron transition with large oscillator strength (0.7884) at ca. 361 nm, which was close to the experimental value (348 nm) and mainly ascribed to the transition from HOMO to LUMO (97%). The transition from HOMO to LUMO did not induce a significant polarity change in ground and excited state. So, energy reduction of excited state after solvent relaxation in polar solvent is not significant, which induces the slight red shifts of the emission wavelength in larger polar solvents.

Luminescence behavior in solid state

First, the fluorescence spectra of the crystals of two compounds were obtained. As shown in Fig. 3, C4MPA had a red-shifted emission band with a maximum at 455 nm relative to that (400 nm) in cyclohexane solution. Therefore, a π-π interaction existed in the crystal phase,[44] which was confirmed by the absorption spectrum of C4MPA. As shown in Fig. 4, a red-shifted absorption band with a maximum peak at 365 nm was observed in C4MPA solid, indicating π-π interaction and a head-to-tail packing between chromophores.[45] The fluorescence quantum yield of C4MPA was determined to be 19% (Table 1), which indicated that C4MPA exhibited an enhanced emission in crystal state. Furthermore, the fluorescence in THF/water (v/v= 1/9) was still very weak, suggesting that the emission enhancement in the crystal should be ascribed to ordered stacking in the crystal phase.[46][47]

To gain further insight into fluorescence enhancement, the crystals was subjected to single-crystal analysis by simple solvent-diffusion method.[41] Colorless block crystals of C4MPA were obtained and the single-crystal structure was successfully analyzed. As shown in Fig. 5a, two kinds of C4MPA with different conformations were found. The two kinds of C4MPA molecules presented different twist angles between the phenyl rings and the cyano or ethylene moieties. The twist angles were between 7.24° and 22.61°, indicating nonplanar conformations.[48] No long-distance close packing was detected, and only dimers consisting of different molecules emerged. Many dimers formed a herringbone packing (Fig. 5b) without extra π-π interaction. Moreover, the distances between two molecules in the dimers were short. For example, the shortest distance between two carbon atoms of the ethylene and phenyl moieties was 3.48 Å. A short distance was observed between the phenyl and oxygen atoms (3.43 Å), which indicated a strong π-π interaction. The large slip angle of ca. 67° between the two C4MPA molecules denoted a *J*-aggregate,[49] which will induce a bathochromic shift of the absorption spectra. In addition, the free rotation of single bonds and isomerization will be suppressed, and an enhanced emission can thus be expected.[50]

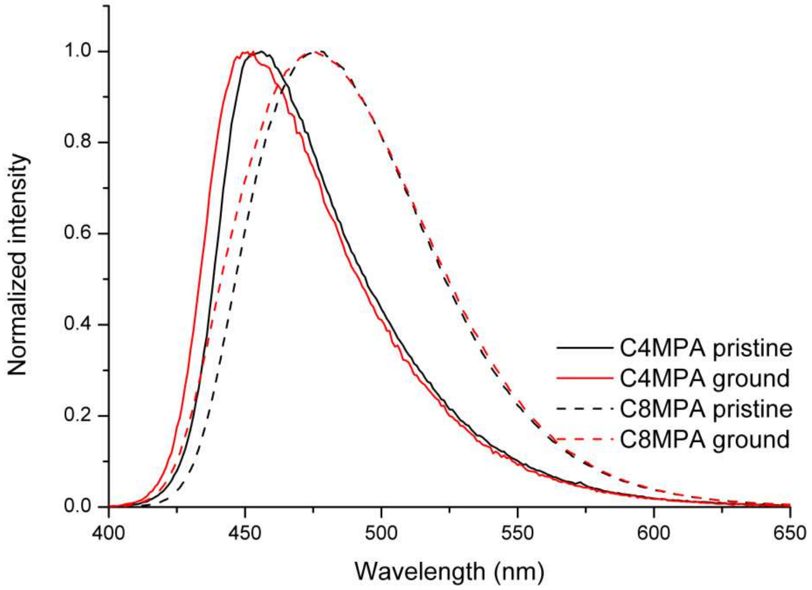

Fig. 3 Normalized fluorescence spectra of C4MPA and C8MPA in pristine and ground states.

Table 1. Photophysical data of C4MPA and C8MPA in crystal phases.

	λ_{abs} (nm)	λ_{em} (nm)	Φ_F (%)	τ (ns)	k_r ($10^9 s^{-1}$)	k_{nr} ($10^9 s^{-1}$)	m.p (°C)
C4MPA	365	455	19	0.67	0.28	0.12	82.5
C8MPA	345, 361	476	76	96.46	0.0079	0.0025	55

The luminescence behavior of C8MPA in crystal state was investigated as well. A rod-like crystal was obtained by solvent-diffusion method. Under 365 nm light, the rod-like crystal emitted a very strong cyan fluorescence, and the fluorescence quantum yield reached 76%. The maximal emission peak was located at 476 nm, suggesting that a π-π interaction probably existed between the chromophores. The single-crystal structure of C8MPA was successfully obtained, and two kinds of molecular conformations existed in the C8MPA crystal.

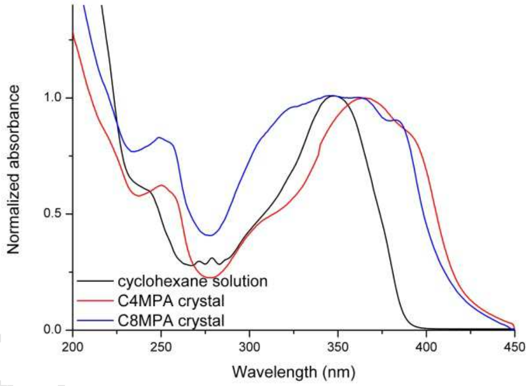

Fig. 4 Normalized absorption spectra of C4MPA in cyclohexane solution and crystal, and C8MPA in crystal.

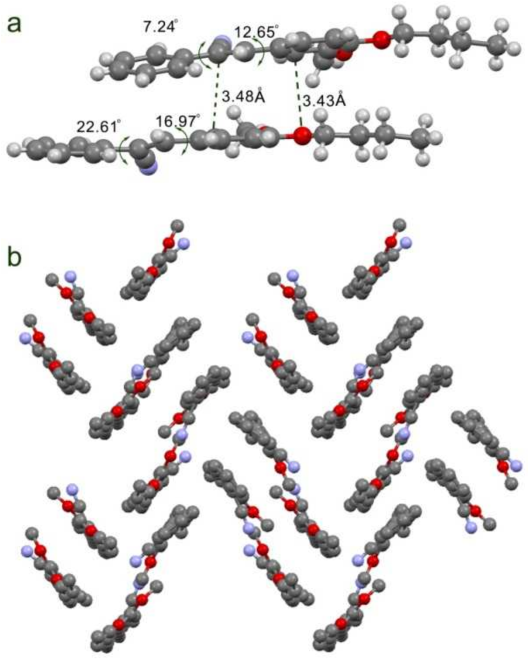

Fig. 5 (a) Dimer of C4MPA with twist angles and the distances between adjacent two molecules, and (b) molecular stacking in crystal phase.

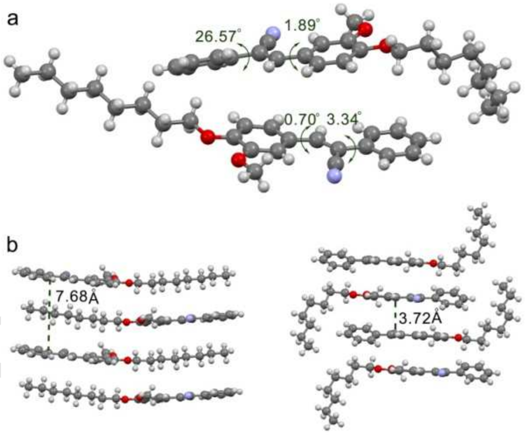

Fig. 6 (a) Dimer of C8MPA with twist angles and the distances between adjacent two molecules, and (b) molecular stacking in crystal phase.

The aromatic moiety of one molecule, named C8MPA-N, adopted nonplanar conformation (Fig. 6a). The twist angle between the terminal phenyl and cyano moieties reaches 26.57°, and the long alkyl chain adopted a folded conformation. The twist angles of the other molecule, named C8MPA-C, were as small as 0.70° and 3.34°, and the alkyl chain was an all-trans configuration.

Moreover, the two kinds of molecules formed individual 1D anti-parallel stacking (Fig. 6b). A long distance of 3.72 Å was observed between the C8MPA-N molecules. By contrast, no effective overlap was found between coplanar C8MPA-C molecules, and the distance between two chromophores of the two adjacent C8MPA-C molecules reached up to 7.68 Å, suggesting the absence of π-π stacking between the C8MPA-C molecules.[51] The absorption spectrum of the C8MPA crystal exhibited a wide band with two maxima at 345 and 361 nm (Fig. 4). The former originated from C8MPA-C in monomolecular state, and the latter was attributed to C8MPA-N in aggregate state. A longer emission wavelength of C8MPA relative to C4MPA implies that C8MPA-C should be responsible for stronger emission because of absence of π-π stacking and a larger conjugation degree.

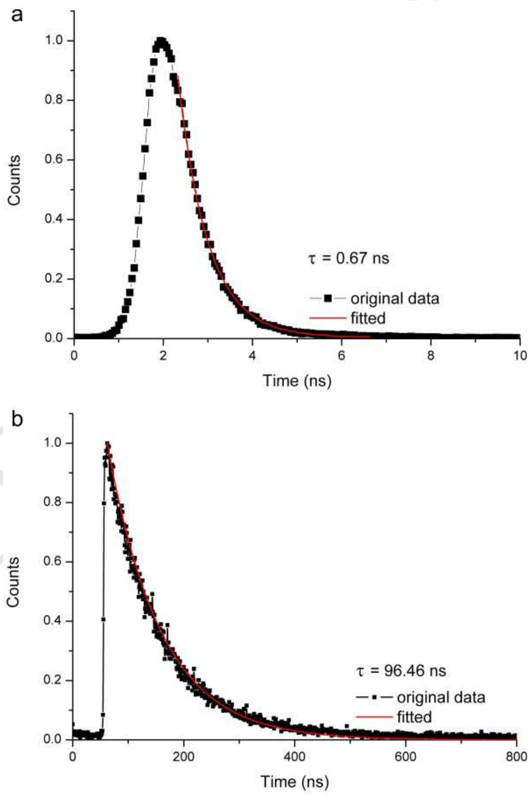

Fig. 7 Time-resolved fluorescence spectra of (a) C4MPA and (b) C8MPA crystals.

To further understand the luminescence difference of the two compounds in crystal state, their time-resolved fluorescence spectra were analyzed. As shown in Fig. 7a and Table 1, the emission decay of C4MPA was single-exponential, and the lifetime was 0.67 ns. Considering a Φ_F of 19%, the radiative rate constant (K_r) was determined to be 0.28×10^9 s^{-1}, and the non-radiative rate constant (K_{nr}) was 0.12×10^9 s^{-1}. In comparison, the decay of the C8MPA fluorescence was extremely slow (Fig. 7b), and the corresponding lifetime reached 96.46 ns. The long lifetime indicated the slow deactivation of excited molecules. K_r was 7.9×10^6 s^{-1}, and K_{nr} was 2.5×10^6 ns^{-1}. Comparison of the K_r and K_{nr} of the two compounds implied that the high Φ_F of C8MPA resulted from the slow non-radiative transition.[52] Combined with the single-crystal structure, coplanar C8MPA-C should be responsible for the higher Φ_F of C8MPA crystals.

Fig. 8 Images of C4MPA in pristine solid state, after shearing by round pen, and then thermal annealing by heating at 70 °C for 5 min.

Luminescence response to mechanical force and thermal stimuli

As suggested by other research teams, cyano ethylene derivatives could exhibit mechanical force-responsive properties. Therefore, their MFC behavior was investigated. As the two compounds had different stacking models in crystal phase, different responsive features to mechanical force stimuli were expected. As shown in Fig. 8, the C4MPA solid film emitted blue fluorescence, and the shearing by a round pen led to a quenched fluorescence stamp. The Φ_F of ground solid decreased to 10%. The maximal emission peak of the sheared solid was located at 450 nm, indicating a blue-shift of only 5 nm (Fig. 3a). The thermal annealing by heating could induce the disappearance of the shearing stamp, thereby indicating a fluorescence recovery. Moreover, the recovered solid film could be stamped again, and such a process could be reversibly repeated many times. The nuclear magnetic resonance spectrum of the shearing solid after shearing-annealing cycles was consistent with the original one, suggesting that the mechanical pressure did not damage the chemical structure.[53] The XRD pattern was measured to investigate the phase transition after the mechanical force stimulus. As shown in Fig. S1a, the pristine solid possessed many sharp and strong diffraction peaks. Similar to those of the pristine solid, the diffraction peaks of the ground solid remained visible, and the peak intensity of only the ground solid weakened. This result suggested that shearing solid only partially destroyed the ordered arrangement of crystals, which may explain why the fluorescence change of C4MPA under mechanical force stimulus was not obvious.[54][55]

The fluorescence response of C8MPA to mechanical force was also investigated. An invisible change in fluorescence color or intensity after grinding was observed by the naked eyes. The fluorescence quantum yield of the ground solid was 75%, and the maximal emission peak was located at 475 nm. The diffraction peaks of the ground solid were similar to those of the pristine solid. Therefore, grinding did not induce a mechanochromism of C8MPA. Interestingly, we found that C8MPA formed supercooling viscous liquid when it was heated at 70 °C and cooled to room temperature, and supercooling liquid was non-emissive (Fig. S2). Such non-emissive viscous liquid kept its liquid state even after 10 h without scarping. It was found that C8MPA started to crystallize when a thin glass rod was used to rub sample. After several minutes whole droplet turned into white solid and emitted very strong fluorescence. Moreover, the C8MPA solid film with an intense cyan fluorescence on a weighing paper lost its fluorescence when heated to 60 °C and a strong cyan fluorescence began to appear after 5 min. The complete recovery of the whole fluorescence required 1 h, suggesting a slow crystallization process too. Such a slow crystallization process was because that the long alkyl chain and the two kinds of molecular conformations in crystal prolonged ordered stacking time. On the other hand, melted C4MPA could change into solid within 2 min when it was cooled to room temperature. Therefore, C8MPA may be used as an excellent thermal responsive fluorescence material.

As shown in Fig. 9, the C8MPA solid film emitted strong fluorescence, and two letters, “TJ”, might be easily written by a hot pen (70 °C). The letters remained visible after 5 min because of the slow crystallization rate and almost disappeared after 15 min. Thus, the information in the film may be automatically erased. Moreover, a new letter might be rewritten by a hot pen, thereby demonstrating a reversible process. Moreover, a regular pattern without fluorescence could be imprinted easily by a hot stamp. When heated using three hot types (70 °C) for 5 s, the fluorescence of the contact region disappeared, and three Chinese characters emerged in the luminescent background. These characters remained visible after 5 min and nearly disappeared after 15 min (Fig. S3). Therefore, such a fluorescence film may be used in temporary information storage or recycled paper. In addition, shearing a melted C8MPA film in a filter paper by mechanical force might accelerate the crystallization process. As shown in Fig. 10, the supercooling film at room temperature was emissive silent. Two Chinese characters with strong cyan fluorescence rapidly appeared along the track of the pen. In view of the slow crystallization speed in other regions without mechanical force shearing, the two characters remained were still visible after 5 min and completely disappeared after 30 min because the crystallization was completed. Moreover, this film could be reused when heated at 70 °C for 2 min.

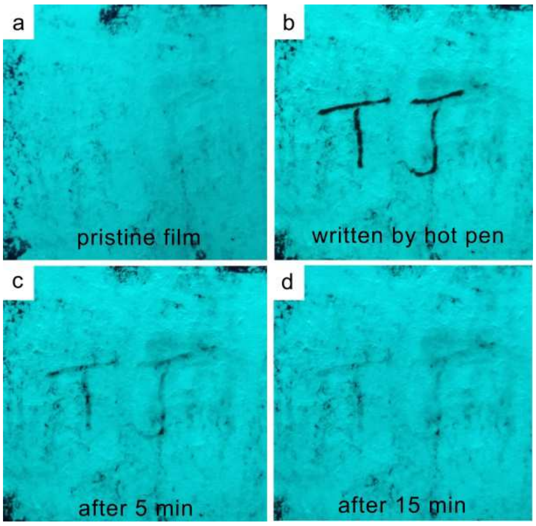

Fig. 9. Photos of C8MPA film in a filter paper under 365 nm light. (a) Pristine solid film, (b) after written “TJ” by a hot pen, naturally left for (c) 5 min and (d) 15 min.

Fig. 10 Photos of supercooling C8MPA filter paper film under 365 nm light. (a) Pristine supercooling film, (b) written by ground pen, naturally left for (c) 5 min and (d) 60 min.

Conclusions

Two cyano-stibene derivatives with different alkyl chains were prepared, and their photophysical properties and response to mechanical force were investigated. Both compounds exhibited a crystallization-induced emission enhancement. They displayed a very weak fluorescence in solution state and emitted an enhanced fluorescence in crystals. C4MPA with a butyl group possessed a 19% Φ_F, and a high Φ_F of 76 % for C8MPA with octyl unit was observed. The single-crystal structure and the time-resolved fluorescence spectra suggested coplanarity, and the 1D sacking in the absence of π-π stacking in C8MPA crystal suppressed the non-radiative transition, which improved the photoluminescence performance. Moreover, they exhibited different responses to mechanical force. The fluorescence of C4MPA was quenched after shearing or grinding, whereas that of C8MPA remained nearly unchanged under mechanical force stimuli. More interestingly, the long alkyl chain endows C8MPA with a low melting point and slow crystallization rate, which make it a promising candidate for optical recording and temperature or force sensing. This work suggests that cyano ethylene moiety is a better building block for constructing intense fluorescence materials, and that the alkyl chain length may endow molecules with distinct properties.

Experimental Section

4.1 Measurements and characterization

The UV-vis spectra were obtained on a Mapada UV-1800pc spectrophotometer. C, H, and N elemental analyses were performed on a PerkinElmer 240C elemental analyzer. Mass spectra were obtained with AXIMA CFR MALDI-TOF (Compact) mass spectrometer. Fluorescence emission spectra were obtained on a FL-3 fluorescence spectrophotometer. The absolute fluorescence quantum yields were measured on an Edinburgh FL-3 steady state spectrometer using an integrating sphere. Luminescent decay experiments were measured on an Edinburgh FL980 spectrometer. EPLED-360 picosecond flash lamp with 898ps pulse duration was used to measure time-resolved fluorescent spectra. NMR spectra were recorded on a Mercury plus 500 MHz instrument. X-ray powder diffraction patterns were obtained on a Bruker D8 ADVANCE X-ray diffractometer equipped with scintillation detector using copper

CuK_α (λ= 1.5406 Å) radiation and a scanning rate of 0.02 s^{-1} (from 5 to 30°). Geometrical optimizations were performed by density functional theory (DFT) calculations at the B3LYP/6-31G level with the Gaussian 09W program package.

Single crystals of C4MPA and C8MPA were obtained by solvent-diffusion (n-hexane/dichloromethane) method and were selected for X-ray diffraction studies in a Rigaku RAXIS-RAPID diffractometer using graphite-monochromated MoK_α radiation (λ= 0.71073 Å). The crystals were kept at room temperature during data collection. The structures were solved by direct methods and refined on F2 by full-matrix least-squares using the SHELXTL-97 program. The C, N, O and H atoms were easily placed from the subsequent Fourier difference maps and refined anisotropically. CCDC 1062078 and 1869506 contain the supplementary crystallographic data for C4MPA and C8MPA.

CnMPA were synthesized by two-step reactions. Synthesis route is shown in Scheme 1. Compound An were synthesized by previously reported procedure.[56] CnPMA were obtained by a condensation reaction in the presence of tetrabutylammonium hydroxide (TBAOH) as catalyst.

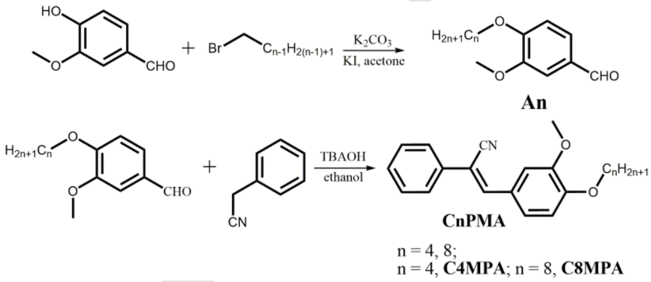

Scheme 1. Synthesis route of CnMPA.

(Z)-3-(4-butoxy-3-methoxyphenyl)-2-phenylacrylonitrile (C4MPA)

A4 (2.0 g, 9.6 mmol), phenylacetonitrile (1.66 mL, 14.4 mmol) and 0.2 mL tetrabutylammonium hydroxide (TBAOH, 40% in water) were added in 20 mL ethanol. The mixture was heated and refluxed for 10 h. The mixture was cooled to room temperature and the solid separated out. The product (2.3 g) was obtained by vacuum suction filtration and washing by cooled ethanol. Yield: 79 %. m.p: 82-83 °C. ^{1}H NMR (500 MHz, $CDCl_3$) 7.73 (d, J = 1.6 Hz, 1H), 7.68 (d, J = 7.5 Hz, 2H), 7.50-7.42 (m, 3H), 7.40 (d, J = 7.2 Hz, 1H), 7.37 (dd, J = 8.4, 1.9 Hz, 1H), 6.94 (d, J = 8.4 Hz, 1H), 4.16-4.03 (m, 2H), 3.98 (s, 3H), 1.96-1.78 (m, 2H), 1.63-1.47 (m, 2H),1.02 (t, J = 7.4 Hz, 3H). MS (MALDI-TOF), m/z: cal: 307.2, found: 307.5. Element analysis (%): calculated for $C_{20}H_{21}NO_2$: C, 78.15; H, 6.89; N, 4.56; Found: C, 78.18; H, 6.82; N, 4.59.

(Z)-3-(3-methoxy-4-(octyloxy)phenyl)-2-phenylacrylonitrile (C8MPA)

By following the synthetic procedure for C4MPA. Yellowish solid (3.0g) was obtained. Yield: 76 %. m.p: 54-56 °C. ^{1}H NMR (500 MHz, $CDCl_3$), 7.71 (d, J = 2.0 Hz, 1H), 7.65 (d, J = 7.5 Hz, 2H), 7.46-7.40 (m, 3H), 7.37 (d, J = 7.3 Hz, 1H), 7.34 (dd, J = 8.4, 2.0 Hz, 1H), 6.92 (d, J = 8.4 Hz, 1H), 4.08 (t, J = 6.9 Hz, 2H), 3.96 (s, 3H), 1.93-1.81 (m, 2H), 1.50-1.40 (m, 2H), 1.41-1.21 (m, 8H), 0.89 (t, J = 6.9 Hz, 3H). MS (MALDI-TOF), m/z: cal: 419.3, found: 419.5. Element analysis (%): calculated for $C_{24}H_{29}NO_2$: C, 79.30; H, 8.04; N, 3.85; Found: C, 79.30; H, 8.04; N, 3.85.

Acknowledgements

This work was supported by the Scientific Research Foundation of Tianjin Normal University (Grant No. 5RL151), the Foundation of Development Program of Future Expert in Tianjin Normal University (WLQR201804) and the Science &Technology Development Fund of Tianjin Education Commission for Higher Education (2018ZD12).

[1] Stuart MAC, Huck WTS, Genzer J, Müller M, Ober C, Stamm M, et al. Emerging applications of stimuli-responsive polymer materials. Nat Mater

2010;9:101.

[2] Tee BC-K, Chortos A, Berndt A, Nguyen AK, Tom A, McGuire A, et al. A skin-inspired organic digital mechanoreceptor. Science (80-) 2015;350:313 LP-316.

[3] Mura S, Nicolas J, Couvreur P. Stimuli-responsive nanocarriers for drug delivery. Nat Mater 2013;12:991.

[4] Zheng B, Wang F, Dong S, Huang F. Supramolecular polymers constructed by crown ether-based molecular recognition. Chem Soc Rev 2012;41:1621–36. doi:10.1039/C1CS15220C.

[5] Sun Y, Wollenberg AL, O'Shea TM, Cui Y, Zhou ZH, Sofroniew M V, et al. Conformation-Directed Formation of Self-Healing Diblock Copolypeptide Hydrogels via Polyion Complexation. J Am Chem Soc 2017;139:15114–21. doi:10.1021/jacs.7b08190.

[6] Foy JT, Li Q, Goujon A, Colard-Itté J-R, Fuks G, Moulin E, et al. Dual-light control of nanomachines that integrate motor and modulator subunits. Nat Nanotechnol 2017;12:540.

[7] Bu L, Sun M, Zhang D, Liu W, Wang Y, Zheng M, et al. Solid-state fluorescence properties and reversible piezochromic luminescence of aggregation-induced emission-active 9,10-bis[(9,9-dialkylfluorene-2-yl)vinyl]anthracenes. J Mater Chem C 2013;1:2028–35. doi:10.1039/C3TC00017F.

[8] Caruso MM, Davis DA, Shen Q, Odom SA, Sottos NR, White SR, et al. Mechanically-Induced Chemical Changes in Polymeric Materials. Chem Rev 2009;109:5755–98. doi:10.1021/cr9001353.

[9] Haehnel AP, Sagara Y, Simon YC, Weder C. Mechanochemistry in Polymers with Supramolecular Mechanophores. In: Boulatov R, editor. Polym. Mechanochemistry, Cham: Springer International Publishing; 2015, p. 345–75. doi:10.1007/128_2015_640.

[10] Xue P, Ding J, Wang P, Lu R. Recent progress in mechanochromism of phosphorescent organic molecules and metal complexes. J Mater Chem C

2016;4:6688–706. doi:10.1039/C6TC01503D.

[11] Chen M, Chen R, Shi Y, Wang J, Cheng Y, Li Y, et al. Malonitrile-Functionalized Tetraphenylpyrazine: Aggregation-Induced Emission, Ratiometric Detection of Hydrogen Sulfide, and Mechanochromism. Adv Funct Mater 2017;28:1704689. doi:10.1002/adfm.201704689.

[12] Liu X, Li M, Liu M, Yang Q, Chen Y. From Tetraphenylfurans to Ring-Opened (Z)-1,4-Enediones: ACQ Fluorophores versus AIEgens with Distinct Responses to Mechanical Force and Light. Chem – A Eur J 2018;24:13197–204. doi:10.1002/chem.201801507.

[13] Ishizuki K, Oka H, Aoki D, Goseki R, Otsuka H. Mechanochromic Polymers That Turn Green Upon the Dissociation of Diarylbibenzothiophenonyl: The Missing Piece toward Rainbow Mechanochromism. Chem – A Eur J 2018;24:3170–3. doi:10.1002/chem.201800194.

[14] Suzuki T, Okada H, Nakagawa T, Komatsu K, Fujimoto C, Kagi H, et al. A fluorenylidene-acridane that becomes dark in color upon grinding – ground state mechanochromism by conformational change. Chem Sci 2018;9:475–82. doi:10.1039/C7SC03567E.

[15] Gong Y-B, Zhang P, Gu Y, Wang J-Q, Han M-M, Chen C, et al. The Influence of Molecular Packing on the Emissive Behavior of Pyrene Derivatives: Mechanoluminescence and Mechanochromism. Adv Opt Mater 2018;6:1800198. doi:10.1002/adom.201800198.

[16] Wan S, Ma Z, Chen C, Li F, Wang F, Jia X, et al. A Supramolecule-Triggered Mechanochromic Switch of Cyclodextrin-Jacketed Rhodamine and Spiropyran Derivatives. Adv Funct Mater 2016;26:353–64. doi:10.1002/adfm.201504048.

[17] Shimogawa H, Yoshikawa O, Aramaki Y, Murata M, Wakamiya A, Murata Y. 4,7-Bis[3-(dimesitylboryl)thien-2-yl]benzothiadiazole: Solvato-, Thermo-, and Mechanochromism Based on the Reversible Formation of an Intramolecular B−N Bond. Chem – A Eur J 2017;23:3784–91. doi:10.1002/chem.201606041.

[18] Zhang F, Zhang R, Liang X, Guo K, Han Z, Lu X, et al. 1, 3-Indanedione functionalized fluorene luminophores: Negative solvatochromism,

nanostructure-morphology determined AIE and mechanoresponsive luminescence turn-on. Dye Pigm 2018;155:225–32. doi:https://doi.org/10.1016/j.dyepig.2018.03.059.

[19] Seki T, Kobayashi K, Ito H. Low-temperature-selective luminescent mechanochromism of a thienyl gold isocyanide complex. Chem Commun 2017;53:6700–3. doi:10.1039/C7CC03190D.

[20] Seki T, Tokodai N, Omagari S, Nakanishi T, Hasegawa Y, Iwasa T, et al. Luminescent Mechanochromic 9-Anthryl Gold(I) Isocyanide Complex with an Emission Maximum at 900 nm after Mechanical Stimulation. J Am Chem Soc 2017;139:6514–7. doi:10.1021/jacs.7b00587.

[21] Walters DT, Aghakhanpour RB, Powers XB, Ghiassi KB, Olmstead MM, Balch AL. Utilization of a Nonemissive Triphosphine Ligand to Construct a Luminescent Gold(I)-Box That Undergoes Mechanochromic Collapse into a Helical Complex. J Am Chem Soc 2018;140:7533–42. doi:10.1021/jacs.8b01666.

[22] Gundu S, Kim M, Mergu N, Son Y-A. AIE-active and reversible mechanochromic tetraphenylethene-tetradiphenylacrylonitrile hybrid luminogens with re-writable optical data storage application. Dye Pigm 2017;146:7–13. doi:https://doi.org/10.1016/j.dyepig.2017.06.043.

[23] Umar S, Jha AK, Purohit D, Goel A. A Tetraphenylethene-Naphthyridine-Based AIEgen TPEN with Dual Mechanochromic and Chemosensing Properties. J Org Chem 2017;82:4766–73. doi:10.1021/acs.joc.7b00456.

[24] Dong Y, Xu B, Zhang J, Tan X, Wang L, Chen J, et al. Piezochromic luminescence based on the molecular aggregation of 9,10-Bis((E)-2-(pyrid-2-yl)vinyl)anthracene. Angew Chemie - Int Ed 2012;51:10782–5. doi:10.1002/anie.201204660.

[25] Xue P, Yao B, Liu X, Sun J, Gong P, Zhang Z, et al. Reversible mechanochromic luminescence of phenothiazine-based 10,10′-bianthracene derivatives with different lengths of alkyl chains. J Mater Chem C

2015;3:1018–25. doi:10.1039/C4TC02126F.

[26] Jiang M, Gu X, Kwok RTK, Li Y, Sung HHY, Zheng X, et al. Multifunctional AIEgens: Ready Synthesis, Tunable Emission, Mechanochromism, Mitochondrial, and Bacterial Imaging. Adv Funct Mater 2017;28:1704589. doi:10.1002/adfm.201704589.

[27] Shen Y, Chen P, Liu J, Ding J, Xue P. Effects of electron donor on luminescence and mechanochromism of D-π-A benzothiazole derivatives. Dye Pigm 2018;150:354–62. doi:10.1016/j.dyepig.2017.12.034.

[28] Xue peng chong, Ding J, Chen P, Wang P, Yao B, Sun J, et al. Mechanical force-induced luminescent enhancement and chromism of a nonplanar D-A phenothiazine derivative. J Mater Chem C 2016;4:5275–80. doi:10.1039/C6TC01193D.

[29] Xue P, Yao B, Sun J, Xu Q, Chen P, Zhang Z, et al. Phenothiazine-based benzoxazole derivates exhibiting mechanochromic luminescence: the effect of a bromine atom. J Mater Chem C 2014;2:3942. doi:10.1039/c4tc00061g.

[30] Jia J, Wu Y. Synthesis, crystal structure and reversible mechanofluorochromic properties of a novel phenothiazine derivative. Dye Pigm 2017;136:657–62. doi:https://doi.org/10.1016/j.dyepig.2016.09.033.

[31] Tan R, Lin Q, Wen Y, Xiao S, Wang S, Zhang R, et al. Polymorphism and mechanochromic luminescence of a highly solid-emissive quinoline-β-ketone boron difluoride dye. CrystEngComm 2015;17:6674–80. doi:10.1039/C5CE01138H.

[32] Louis M, Guillot R, Métivier R, Allain C. β-Diketone derivatives: influence of the chelating group on the photophysical and mechanofluorochromic properties. Photochem Photobiol Sci 2018;17:822–8. doi:10.1039/C8PP00070K.

[33] Yoshii R, Nagai A, Tanaka K, Chujo Y. Highly Emissive Boron Ketoiminate Derivatives as a New Class of Aggregation-Induced Emission Fluorophores. Chem – A Eur J 2013;19:4506–12. doi:10.1002/chem.201203703.

[34] Wang Y, Xu D, Gao H, Wang Y, Liu X, Han A, et al. Twisted Donor–Acceptor Cruciform Luminophores Possessing Substituent-Dependent Properties of

Aggregation-Induced Emission and Mechanofluorochromism. J Phys Chem C 2018;122:2297–306. doi:10.1021/acs.jpcc.7b11368.

[35] Luo J, Xie Z, Lam JWY, Cheng L, Chen H, Qiu C, et al. Aggregation-induced emission of 1-methyl-1,2,3,4,5-pentaphenylsilole. Chem Commun 2001:1740–1. doi:10.1039/B105159H.

[36] Hong Y, Lam JWY, Tang BZ. Aggregation-induced emission. Chem Soc Rev 2011;40:5361. doi:10.1039/c1cs15113d.

[37] Zhao J, Chi Z, Yang Z, Mao Z, Zhang Y, Ubba E, et al. Recent progress in the mechanofluorochromism of distyrylanthracene derivatives with aggregation-induced emission. Mater Chem Front 2018;2:1595–608. doi:10.1039/C8QM00130H.

[38] Machida T, Taniguchi R, Oura T, Sada K, Kokado K. Liquefaction-induced emission enhancement of tetraphenylethene derivatives. Chem Commun 2017;53:2378–81. doi:10.1039/C6CC09939D.

[39] Chung K, Kwon MS, Leung BM, Wong-Foy AG, Kim MS, Kim J, et al. Shear-Triggered Crystallization and Light Emission of a Thermally Stable Organic Supercooled Liquid. ACS Cent Sci 2015;1:94–102. doi:10.1021/acscentsci.5b00091.

[40] Zheng X, Zheng Y, Peng L, Xiang Y, Tong A. Mechanoresponsive Fluorescence of 2-Aminobenzophenone Derivatives Based on Amorphous Phase to Crystalline Transformation with High "Off–On" Contrast Ratio. J Phys Chem C 2017;121:21610–5. doi:10.1021/acs.jpcc.7b06920.

[41] Hariharan PS, Gayathri P, Moon D, Anthony SP. Tunable and Switchable Solid State Fluorescence: Alkyl Chain Length-Dependent Molecular Conformation and Self-Reversible Thermochromism. ChemistrySelect 2017;2:7799–807. doi:10.1002/slct.201701550.

[42] Xue P, Yao B, Sun J, Zhang Z, Lu R. Emission enhancement of a coplanar π-conjugated gelator without any auxiliary substituents. Chem Commun (Camb) 2014;50:10284–6. doi:10.1039/c4cc04869e.

[43] Dou C, Han L, Zhao S, Zhang H, Wang Y. Multi-Stimuli-Responsive

Fluorescence Switching of a Donor−Acceptor π-Conjugated Compound. J Phys Chem Lett 2011;2:666–70. doi:10.1021/jz200140c.

[44] Xue P, Yang Z, Chen P. Hiding and revealing information using the mechanochromic system of a 2,5-dicarbazole-substituted terephthalate derivative. J Mater Chem C 2018;6:4994–5000. doi:10.1039/c8tc01379a.

[45] Rösch U, Yao S, Wortmann R, Würthner F. Fluorescent H-aggregates of merocyanine dyes. Angew Chemie - Int Ed 2006;45:7026–30. doi:10.1002/anie.200602286.

[46] Nirmalananthan N, Behnke T, Hoffmann K, Kage D, Gers-Panther CF, Frank W, et al. Crystallization and Aggregation-Induced Emission in a Series of Pyrrolidinylvinylquinoxaline Derivatives. J Phys Chem C 2018;122:11119–27. doi:10.1021/acs.jpcc.8b01425.

[47] Xue P, Ding J, Shen Y, Gao H, Zhao J, Sun J, et al. Aggregation-induced emission nanofiber as a dual sensor for aromatic amine and acid vapor. J Mater Chem C 2017;5:11532–41. doi:10.1039/c7tc03192k.

[48] Desroches M, Morin J-F. Anthanthrene as a Super-Extended Tetraphenylethylene for Aggregation-Induced Emission. Org Lett 2018;20:2797–801. doi:10.1021/acs.orglett.8b00452.

[49] Würthner F, Kaiser TE, Saha-Möller CR. J-Aggregates: From Serendipitous Discovery to Supramolecular Engineering of Functional Dye Materials. Angew Chemie Int Ed 2011;50:3376–410. doi:10.1002/anie.201002307.

[50] Zhang C-J, Feng G, Xu S, Zhu Z, Lu X, Wu J, et al. Structure-Dependent cis/trans Isomerization of Tetraphenylethene Derivatives: Consequences for Aggregation-Induced Emission. Angew Chemie Int Ed 2016;55:6192–6. doi:10.1002/anie.201600244.

[51] Banerjee M, Emond SJ, Lindeman S V, Rathore R. Practical Synthesis of Unsymmetrical Tetraarylethylenes and Their Application for the Preparation of [Triphenylethylene−Spacer−Triphenylethylene] Triads. J Org Chem 2007;72:8054–61. doi:10.1021/jo701474y.

[52] Li G, Nobuyasu RS, Zhang B, Geng Y, Yao B, Xie Z, et al. Thermally

Activated Delayed Fluorescence in CuI Complexes Originating from Restricted Molecular Vibrations. Chem – A Eur J 2017;23:11761–6. doi:10.1002/chem.201701862.

[53] Oda K, Hiroto S, Shinokubo H. NIR mechanochromic behaviours of a tetracyanoethylene-bridged hexa-: Peri-hexabenzocoronene dimer and trimer through dissociation of C-C bonds. J Mater Chem C 2017;5:5310–5. doi:10.1039/c7tc01270e.

[54] Xue P, Sun J, Chen P, Gong P, Yao B, Zhang Z, et al. Strong solid emission and mechanofluorochromism of carbazole-based terephthalate derivatives adjusted by alkyl chains. J Mater Chem C 2015;3:4086–92. doi:10.1039/C5TC00267B.

[55] Liu Z, Zhang K, Sun Q, Zhang Z, Tang L, Xue S, et al. Synthesis and remarkable mechano- and thermo-hypsochromic luminescence of a new type of DPP-based derivative. J Mater Chem C 2018;6:1377–83. doi:10.1039/C7TC04698G.

[56] Muškinja J, Burmudžija A, Ratković Z, Ranković B, Kosanić M, Bogdanović GA, et al. Ferrocenyl chalcones with O-alkylated vanillins: synthesis, spectral characterization, microbiological evaluation, and single-crystal X-ray analysis. Med Chem Res 2016;25:1744–53. doi:10.1007/s00044-016-1609-8.

1. Two cyano-stilbene derivatives exhibited crystallization-induced emission enhancement.
2. Crystal stacking models of two compounds are different.
3. Supercooling liquid C8MPA emitted enhanced fluorescence after shearing.